



OPEN Research on multi-objective optimization design for high-precision turning-milling machine tool bed based on taguchi method -FEA

Hongyi Wu¹, Haozhen Li¹, Xuanyi Wang^{1,3}, Junshou Yang¹, Runze Jiang¹, Xiaolei Deng^{2✉} & Jianchen Wang¹

As a high-precision machining equipment, the turning-milling machine tool requires its bed structure the primary load-bearing component to exhibit excellent dynamic and static characteristics that significantly influence machining accuracy and efficiency. To ensure machining precision, this paper proposes a multi-objective collaborative optimization design methodology integrating Finite Element Analysis (FEA) and Taguchi Method. This approach employs FEA technology to obtain the static and dynamic characteristics of the machine tool bed (MTB) structure, followed by multi-objective collaborative optimization using Taguchi Method to achieve comprehensive performance enhancement. Compared with the traditional research methods for optimizing machine tool beds, the FEA technology can handle more complex geometric shapes and boundary conditions, improve the accuracy and reliability of data, and enhance the optimization efficiency through the Taguchi method, achieving multi-objective joint optimization. Comparative analysis demonstrates that the optimized structure achieves 5.14% reduction in maximum deformation, 1.75% decrease in mass, and 1.04% improvement in fourth-order natural frequency. The results validate the effectiveness of this design methodology in achieving efficient MTB optimization for turning-milling machine tools, simultaneously enhancing dynamic-static performance while realizing lightweight design. This research provides valuable references for advancing precision improvement and green manufacturing research in turning-milling machine tools.

Keywords High-precision turning-milling machine tool, Machine tool bed, Multi-objective joint optimization, Lightweight design, Taguchi method

As the core carrier of high-end CNC equipment, the performance of turning-milling machine tool directly determines the precision of complex parts machining and the efficiency of multi-process integration¹. The machine tool bed (MTB), as the basic support unit of the machine tool (MT), not only needs to withstand cutting force, inertia force of moving parts and other sources of load, but also needs to maintain structural stability under dynamic working conditions, and its mechanical properties directly affect the positioning accuracy of the whole machine and machining surface quality. Therefore, it is necessary to optimize the dynamic and static characteristics of the machine tool bed and carry out lightweight design. The improvement of rigidity can effectively enhance the machining accuracy and stability of the machine tool while reducing the impact of thermal deformation, while lightweight design can lower the energy consumption and operating costs of product manufacturing.

The traditional MTB design commonly uses a combination of analogue design and empirical formulae correction, which can ensure the basic load carrying requirements, but often leads to structural redundancy and material over-distribution². Studies have shown that over-reliance on the safety factor design strategy will cause a significant increase in the mass of the MTB, which not only causes a waste of resources, but also exacerbates

¹Key Laboratory of Intelligent Manufacturing for Aerodynamic Equipment of Zhejiang Province, Quzhou University, Quzhou 324000, China. ²College of Mechanical Engineering, Jiaying University, Jiaying 314001, China. ³College of Mechanical Engineering, Zhejiang University of Technology, Hangzhou 310032, China. ✉email: dxl@zju.edu.cn

the nonlinear characteristics of the dynamic response of the MT. With the increasingly stringent requirements of high-speed precision machining on the power density and dynamic characteristics of MT, how to optimize the dynamic performance and achieve lightweight while ensuring static stiffness³ has become a key technological bottleneck to enhance the core competitiveness of MT. The current transformation and upgrading of the manufacturing industry put forward higher requirements for MT equipment, not only to meet the dynamic stability of high acceleration movement, but also need to meet the green manufacturing concept of energy efficiency standards. The traditional casting MTB has low material utilization and other problems, and it is difficult to adapt to the design requirements of multi-objective co-optimisation, so it is necessary to optimize the MTB structure and carry out multi-objective optimisation design of stiffness-quality-dynamic characteristics. In the global industrial context, companies are constantly looking for new design solutions to improve the quality of manufactured products, reduce the costs associated with the manufacturing process, increase the flexibility of the process⁴.

In recent years, research on machine tool performance optimization has shown a trend of deep integration of multi-disciplinary methods. Finite element analysis (FEA), as a core technology, is often combined with intelligent optimization algorithms, dynamic modeling, and experimental design methods to form an efficient hybrid optimization framework, thereby enhancing the dynamic and static stiffness, accuracy, and vibration control capabilities of machine tools. In terms of structural design and dynamic performance optimization, researchers generally adopt FEA combined with intelligent algorithms. Minh et al.⁵ proposed an innovative method that combined the pseudo-rigid body model, Lagrangian dynamics and FEA, and introduced the crayfish optimization algorithm to optimize the XY flexible positioner design, significantly increasing the natural frequency. It was successfully applied to vibration-assisted milling and improved surface roughness. Chen et al.⁶ utilized BP neural network and genetic algorithm to conduct multi-objective optimization on five-axis tool grinding machines. Through FEA parametric analysis and neural network fitting, the machine tool deformation was reduced by 21% and the natural frequency was increased by 6–9%. In the field of dynamic modeling and real-time analysis, hybrid methods have addressed the bottleneck of computational efficiency. Kim et al.⁷ developed a flexible multi-body dynamics model based on modal state space simplification, combined with FEA to achieve real-time vibration analysis of digital twins, with a prediction accuracy rate of 88%. Park et al.⁸ introduced machine learning and computer vision to predict the dynamics of the blade tip based on finite element simulation and sensory coupling methods, providing a new approach for flutter suppression. Precision compensation and error control both benefit from algorithm fusion. Yasser et al.⁹ proposed a geometric error compensation framework based on particle swarm optimization, combining inverse kinematics and collision detection to optimize the trajectory accuracy of five-axis machine tools and highlight the advantages of meta-heuristic algorithms in handling nonlinear errors.

In addition, the research on lightweight design of machine tools has shown the characteristics of multi-technology integration and multi-disciplinary intersection. Relevant international scholars have mainly explored from three dimensions: material innovation, structural optimization and performance improvement. In terms of material substitution, Li's team¹⁰ adopted resin concrete to replace traditional castings, achieving weight reduction while ensuring dynamic and static characteristics. Li et al.¹¹ reduced the total weight of components by 37.9% through integrated design, demonstrating the potential for collaborative optimization of materials and structures. Structural bionic design has become an important direction. Hu et al.¹² drew on the biological honeycomb structure and achieved lightweight of the workbench through the arrangement of irregular circular tubes, demonstrating the application value of bionics in the engineering field. The structural optimization methods show a diversified trend. Xu et al.¹³ used the finite element displacement method to improve the stiffness and accuracy of the spinning machine. Deng's team¹⁴ optimized the dynamic stiffness configuration of the joint based on the orthogonal test method and established a quantitative relationship between the test design and dynamic performance. Liu et al.¹⁵ proposed a quadratic optimization method including zero-order optimization and parameter rounding, achieving the efficient lightweight of the gantry frame structure. In terms of the application of intelligent algorithms, Xin et al.¹⁶ adopted the NSGA-II algorithm to complete the multi-objective optimization of the gearbox housing, achieving noise reduction and environmental protection while reducing the weight by 434 kg. Xiao et al.¹⁷ innovatively introduced particle damping technology and verified the synergistic effect of dynamic vibration reduction and lightweight through experiments. At the level of performance maintenance and improvement, Chan et al.¹⁸ achieved the dual goals of lightweight and natural frequency enhancement through structural deformation control, revealing the importance of mechanical property balance in lightweight design. These studies indicate that modern lightweight design has shifted from simple weight reduction to performance-driven system optimization, emphasizing the collaborative innovation of materials, structures and processes. The future development trend will place greater emphasis on the integration of multi-disciplinary methods, precise control of dynamic characteristics, and in-depth application of intelligent optimization algorithms, providing technical support for achieving efficient and energy-saving green manufacturing equipment.

Taguchi method as a local optimal design method is distinguished from other local optimal design methods by its ability to achieve multi-objective optimal design, which can be searched for the best combinations during multi-objective optimal design in a minimum number of experiments by building orthogonal tables. As early as 2002, Fazilat et al.¹⁹ in the field of biomechanics combined finite element model modelling with robust parameter design of Taguchi method to incorporate uncertainty in the model. Layeb et al.²⁰ used Taguchi method to determine the optimal design structure and performed finite element analysis to validate the optimisation process. Verim et al.²¹ adopted Taguchi analysis to streamline the number of experiments and determine optimal printing parameters for maximizing the mechanical performance of printed materials. Satpute et al.²² employed the Taguchi method to determine ideal operating parameters for a solar thermal collector with a rectangular spiral absorber, establishing optimum conditions for enhancing the system's electrical and thermal efficiency.

In this paper, a multi-objective optimisation method integrating the finite element method and Taguchi test method is proposed for the demand of dynamic and static performance improvement of the MTB of turning-milling MT. By constructing a parametric finite element model of the MTB for static and dynamic characteristic analysis, combining with orthogonal test design to screen the key design variables, and establishing the optimisation function with the objectives of mass reduction, maximum deformation reduction and low-order intrinsic frequency enhancement. The signal-to-noise ratio analysis and variance test are used to determine the optimal parameter combinations, and the synergistic optimisation effect of mass reduction, fourth-order intrinsic frequency enhancement, and shape variable reduction in the key parts of the MTB is finally achieved.

Optimisation methods and solutions for MTB MTB characterization method

With the rapid development of today's CAE technology, in the field of industrial design, in order to pursue a higher quality of product design and more reasonable product design structure, the finite element method has been widely used in the field of structural design. Through the finite element analysis software on the more rough design structure for finite element simulation²³, through the imposition of the actual working conditions of the boundary conditions, to get the structure of the performance parameters, based on which to achieve a more detailed structural design.

Finite element analysis is a numerical method for solving engineering and scientific problems by decomposing complex structures into smaller, interconnected units. In FEA, a continuum (e.g., a solid, shell, or frame) is first divided into a finite number of discrete units that are interconnected by nodes. Simple geometrical shapes (e.g. triangles, quadrilaterals, tetrahedron, etc.) are assumed inside each cell and mathematical models are constructed based on these simple shapes. This discretisation process not only simplifies the problem but also permits the use of numerical methods to solve complex continuum problems. In order to derive the mathematical equations from each cell, it is necessary to choose appropriate approximation functions to describe the unknown field variables within the cell. Boundary conditions specify constraints such as displacements, velocities, or forces on the structure at the boundary; while initial conditions describe the state at the beginning of the analysis, such as the initial stress distribution, temperature distribution, etc. The correct imposition of these conditions is essential to obtain accurate analysis results. The continuous evolution of finite element analysis technology has not only reconfigured the traditional mechanical design process, but also spawned new modes of intelligent manufacturing, such as digital twin and virtual verification, which continue to promote the evolution of industrial products in the direction of high performance and high reliability.

MTB optimisation methods

Taguchi method

Taguchi method was founded by Dr. Genichi Taguchi in Japan, and it is a quality engineering method that can improve the quality of product design in a cost-effective way, which consists of five steps: selecting the design features, determining the design factors, setting the optimisation level, designing the orthogonal test table, and analyzing and verifying the experimental design. Taguchi method evaluates the target quality through the signal-to-noise(S/N) ratio, and the larger the S/N ratio, the better the design results²⁴. And the signal-to-noise ratio is calculated by different formulas in different cases, which are Larger is better “(S/N)₁”, Nominal is better “(S/N)₂” and Smaller is better “(S/N)₃”. The different S/N calculation formulas have significant differences and corresponding advantages. The corresponding formula is:

$$\begin{cases} (S/N)_1 = 10 \log\left(\frac{1}{n} \sum_{i=1}^n y_i^2\right) \\ (S/N)_2 = 10 \log(\bar{y}^2 / \hat{\sigma}^2) \\ (S/N)_3 = -10 \log\left(\frac{1}{n} \sum_{i=1}^n y_i^2\right) \end{cases} \quad (1)$$

where n is the overall sample size; y_i is the test sample; $\hat{\sigma}$ is the sample standard deviation; and \bar{y} is the sample mean.

Taguchi tests can be used to screen the parameters for optimisation, reduce the number of parameter tests, and improve the quality and effectiveness of parameter tests, which can reduce the design cycle time and significantly improve the optimisation efficiency²⁵.

Multi-objective joint optimisation approach

Based on the multi-objective optimisation theory, a mathematical model of multi-objective optimisation is established, and the mass, maximum deformation and low-order intrinsic frequency of the MTB are taken as the optimisation objectives. Among them, machine deformation, as a key variable affecting machining accuracy, leads to structural deformation under the action of cutting force and thermal stress, which directly triggers dimensional deviation, vibration aggravation and tool wear, and is the core bottleneck restricting the stability of the MT, and it has become the core technological path for high-end MT to break through the accuracy limit. The deformation is solved by the finite element model, and its stiffness matrix equation is.

$$[K] \{u\} = \{F\} \quad (2)$$

where $[K]$ is the global stiffness matrix; $\{u\}$ is the nodal displacement vector; $\{F\}$ is the nodal force vector. By meshing the model and setting the boundary conditions, the above stiffness matrix equation is solved to obtain $\{u\}$, and finally the deformation magnitude can be obtained through processing.

In addition, the intrinsic frequency of the MT, as an inherent property of the MT system itself, is a parameter that needs to be optimised at the design stage of the MT, and in the process of using the MT, it is necessary to avoid its overlap with the frequency of the external excitation, and to monitor the trend of its change when maintaining the machine, and the stability of the MT directly determines its reliability, machining accuracy and service life. The corresponding formula is:

$$f_n = \frac{1}{2\pi} \sqrt{\frac{k}{m}} \quad (3)$$

where f_n is the desired intrinsic frequency; k is the stiffness of the MT structural system; and m is the mass of the system.

Select a good design solution and set the selection range of its solution, which can be expressed as:

$$\begin{cases} \min [m(X), f_d(X), -f_f(X)] \\ X = [x_1, x_2, x_3, \dots, x_j, \dots, x_n]^T \\ f_d(X) \leq f_d(X)_0 \\ f_f(X) \geq f_f(X)_0 \\ A_j \leq x_j \leq B_j \end{cases} \quad (4)$$

where $m(X)$ is the mass of MTB; $f_d(X)$ is the maximum static deformation after optimisation; $f_d(X)_0$ is the maximum static deformation of the original MT; $f_f(X)$ is the optimised fourth order intrinsic frequency; $f_f(X)_0$ is the fourth order intrinsic frequency of the original MT; A_j and B_j are the upper and lower limits of the j th design variable, respectively; x_j is the corresponding value of the j th design variable.

The mathematical model can provide diversified results by considering multiple objectives. And it can also make trade-offs between different objectives to avoid pursuing a single objective too much and neglecting other objectives, and can achieve the selection of the optimal scheme from a large number of different improvement schemes. The flow chart of the multi-objective joint optimisation scheme based on the finite element-Taguchi method is shown in Fig. 1.

MTB modelling and static and dynamic performance analysis

Simplification of the MTB model

The MTB of the high-precision turning-milling MT studied in this paper is mainly composed of reinforcement, rib plate, spindle load-bearing table, turret load-bearing table, motor load-bearing table and tool holder.

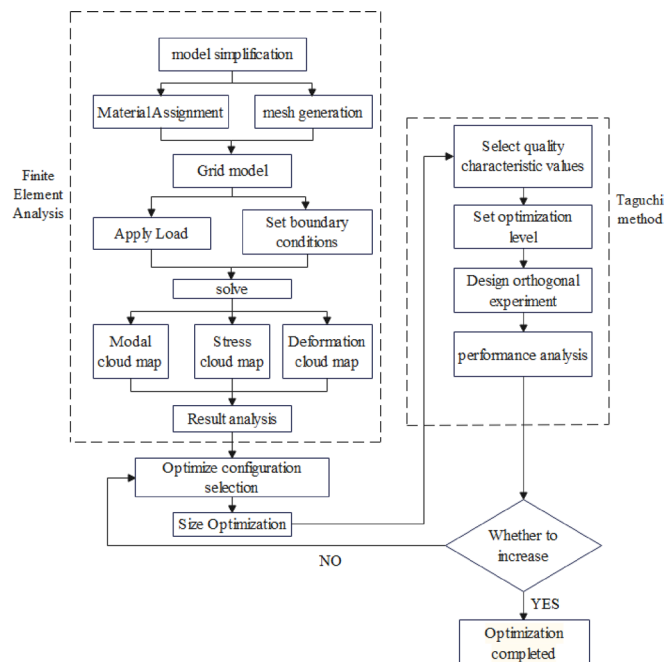


Fig. 1. Flow chart for MTB optimisation.

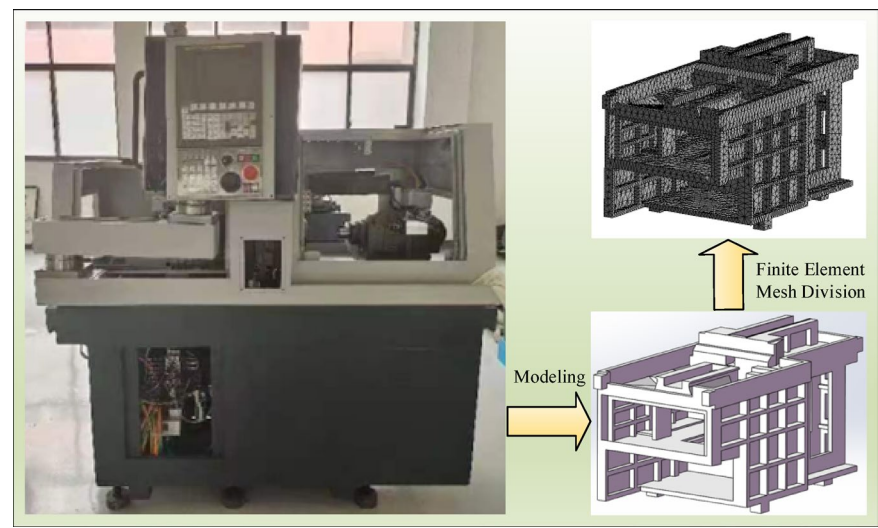


Fig. 2. Establishment of MTB model and grid division.

Mesh Type	Mesh Size	Number of units	Number of nodes
Triangle	20 mm	71,565	134,502

Table 1. Mesh-related parameters.

The material of the MTB is made of Grey cast iron HT300, with a density of 7,300 kg/m³, a modulus of elasticity of 143GPa, a Poisson's ratio of 0.27, a permissible stress of 335 MPa, and an overall mass of 1273 kg. Since the MTB structure is more complicated, appropriate model simplification should be made when the MTB structure is drawn and modeled. In the finite element calculation, part of the small size features may cause the mesh quality is too low, affecting the accuracy of the simulation analysis, the simulation results have little effect, usually can delete this kind of size to ensure the quality of the mesh, the initial simplified MTB modelling as shown in Fig. 2.

Finite element modelling of the MTB

Before the design optimisation, the original MTB structure is analyzed for dynamic and static characteristics. The static and vibration characteristics are analyzed by finite element simulation technology, and the dynamic and static characteristic indexes such as deformation displacement, equivalent force and intrinsic frequency of the MTB are obtained. The deficiencies of the MTB structure and the location of excessive material redundancy are identified to provide guidance and basic evaluation criteria for the subsequent multi-objective optimisation design.

Finite element mesh division

The 3D model of the MTB is imported into ANSYS software, and the model is pre-processed for finite element analysis, including defining material properties, meshing, setting boundary conditions, etc. After a number of experiments on the mesh type and size adjustment, found that when the mesh size down to 20 mm, whether it is the MTB plane position or depression position and bending position, the stress changes are larger, more detailed. Meanwhile, through grid independence analysis, the grid sizes selected for comparison were 20 mm and 14 mm respectively. Through simulation analysis, the deformations obtained were 10.017 μm and 10.166 μm respectively, with a difference of approximately 1.5% and less than 5%, so this paper selects 20 mm as the mesh size. At the same time, simplify the MTB model on the chamfer, camber and other features that have a small impact on the analysis results, reducing the difficulty of mesh division, and improve the efficiency of the operation. Mesh-related parameters are shown in Table 1.

Boundary condition

The main loads come from its own gravity and the pressure of other parts installed on the MTB, which mainly include the turret load-bearing table(F1), motor load-bearing table(F2), tool holder(F3) and spindle load-bearing table(F4). When conducting the analysis, as the quality of each component may vary under different working conditions, the actual weight of the components obtained from the actual mapping is simplified to reduce unnecessary workload in the subsequent analysis process. At the same time, fixed constraints are applied at the load-bearing base. The location and magnitude of the loads on the MTB are shown in Fig. 3 below:

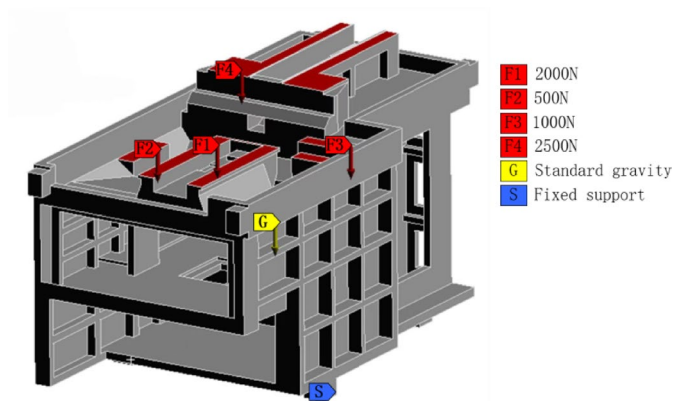


Fig. 3. MTB load distribution.

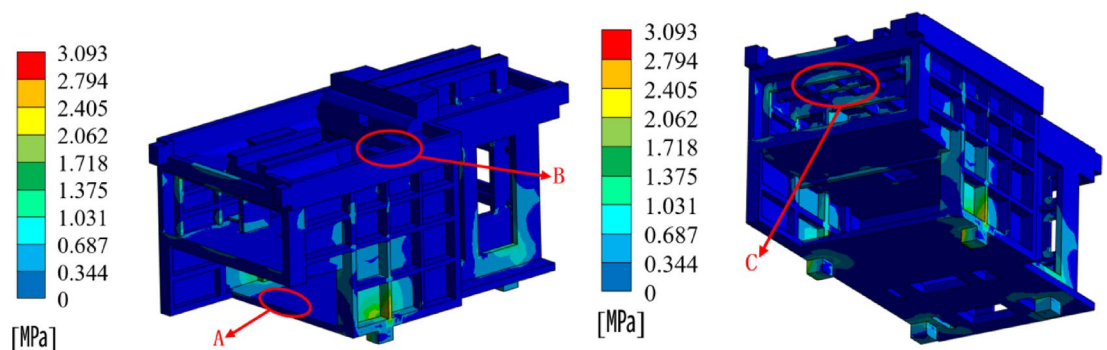


Fig. 4. The stress contour of MTB.

Static and dynamic performance analysis of MTB

Static characterization

The static characteristic analysis of the MTB is the core link to ensure the machining accuracy and stability of CNC, and it accurately evaluates the deformation and stress distribution of the guide rail, load-bearing slide rail and other key parts under load through static simulation. As the guide rail deformation directly affects the accuracy of the tool trajectory, millimetre-level deviation can lead to multiplication of work-piece machining error, so the static stiffness analysis becomes a key basis for balancing material reduction and structural performance in lightweight design, to ensure that the optimised MTB maintains sufficient deformation resistance at the same time as weight reduction, avoiding vibration or precision degradation due to insufficient stiffness, and fundamentally support the MT's high-precision, long-life operation requirements.

The static characteristics of the MTB are analyzed and the stress contour is shown in Fig. 4 and the deformation contour is shown in Fig. 5.

The analysis results show that the maximum equivalent stress of the MTB is 3.09 MPa, and the maximum deformation is about 10.02 μm . Under the static load, the deformation is within the permissible range, and the maximum stress level is much smaller than the permissible stress, so the original design meets the requirements for the use of the MTB. As can be seen from Fig. 5, the main deformation of the MTB is reflected in A, B and C in the figure, in which the deformation in A and B is smaller and the equivalent stress is much smaller than the permissible stress of the material in this place, indicating that there is a certain amount of optimisation space for the lightweighting of the MTB in this place, while C in the figure is the largest place of deformation, and its deformation is in the permissible range.

The turning-milling MT, as high-precision MT, have more stringent rigidity requirements for their bed guides. When the maximum deformation is close to the critical value, it may potentially affect the accuracy of the work-piece involved in the machining process of the MT. In order to assess the deformation of the bed guides, a static analysis of the bed guides was carried out. The deformation contour diagram and the corresponding deformation curve of the bed guides of the precision vertical coordinate boring machine are shown in Fig. 6.

As shown in Fig. 6(a), the deformation of the bed guides is more significant near the table position, while the deformation at the front and rear ends is smaller. Figure 6(b) shows the Z-direction deformation curve of the guideway before optimisation, and the maximum deformation value of the bed guides is 10.017 μm , and the minimum value is 8.922 μm , which reflects the rigidity performance of the bed guides under the working condition.

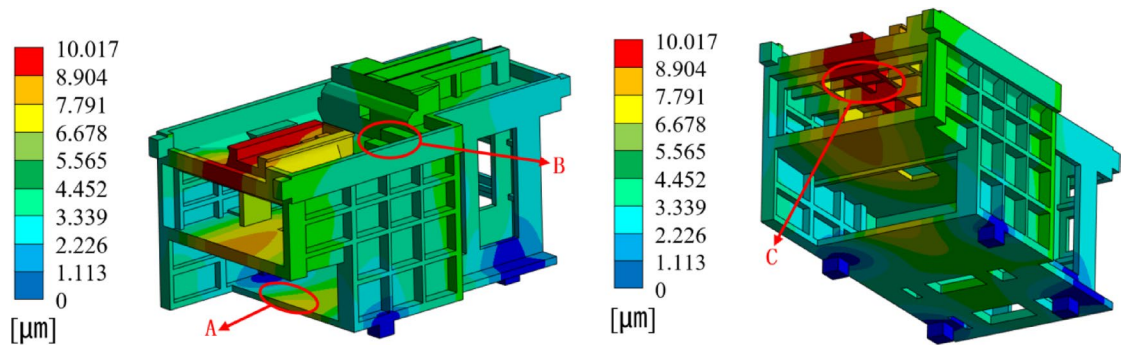


Fig. 5. The deformation contour of MTB.

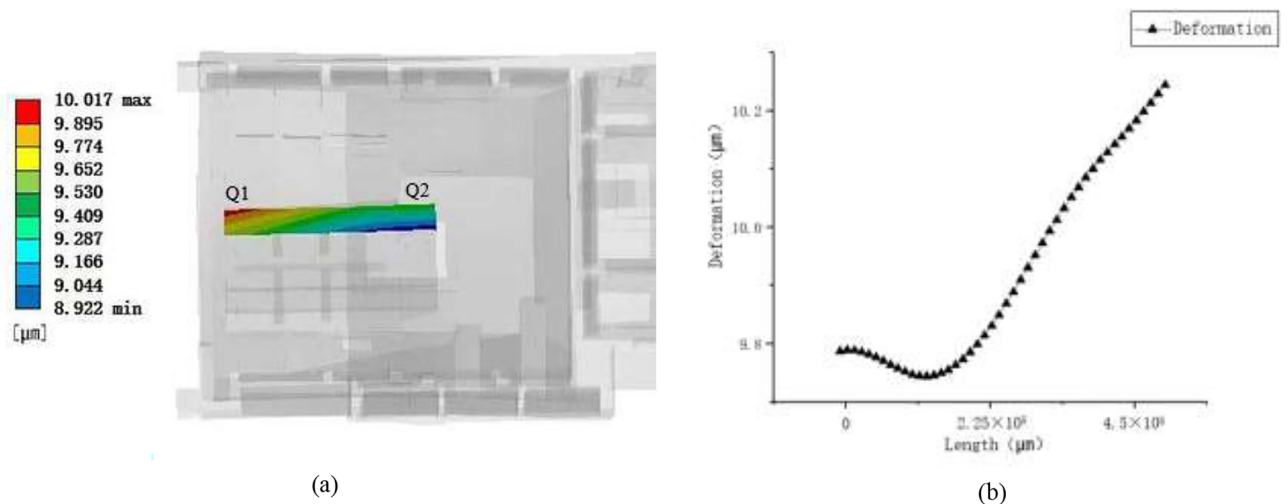


Fig. 6. Deformation contour diagram and corresponding deformation curve of bed guides: (a) Deformation contour diagram of bed guides; (b) Deformation curve of the bed guide rail in the Q2-Q1 direction.

In summary, although the original design indicators are within the permissible range, it may potentially affect the accuracy of the work-piece involved in the machining process of the MT, especially in the case of prolonged operation or high load conditions, the guide rails of machine tools will gradually undergo slight deformation. The impact of this on the machining accuracy of the machine tool mainly includes affecting the straightness error of the guide rails, affecting the parallelism error of the guide rails, and causing the guide rails to twist. Under the influence of these, the relative position between the tool and the workpiece will undergo subtle changes during operation, which will directly affect the machining accuracy of the workpiece, which may exacerbate the deformation of the MT, thus affecting the machining quality and machining accuracy. Therefore, it is all the more necessary to carry out structural optimisation here to improve structural rigidity and reduce MTB deformation, thereby enhancing the overall mechanical properties of the MT.

Modal analysis

Modal analysis of the MTB is a key technology to ensure the dynamic stability of CNC, and its core lies in the accurate identification of the intrinsic frequency of the structure to avoid the risk of resonance. The intrinsic frequency, as the core parameter of the system to resist external excitation, is directly determined by the structural dimensions, mass distribution and stiffness characteristics, and it is the basic index to assess the vibration resistance of the MT^{26,27}.

During machine operation, if the periodic excitation frequency generated by the cutting force, spindle rotation or feed system coincides with the intrinsic frequency of the MTB, resonance phenomena will be triggered, leading to tool trajectory deviation, deterioration of work-piece surface quality and even fatigue failure of key components. By quantifying the intrinsic frequency of the MTB through modal analysis, the structural parameters can be pre-adjusted at the design stage to raise the intrinsic frequency outside the excitation band. Especially in lightweight design, the intrinsic frequency should not be degraded as a prerequisite constraint to ensure the balance between weight reduction and dynamic performance. Therefore, modal analysis is not only a necessary means to prevent resonance and improve machining accuracy, but also a core guarantee to achieve

high reliability and long life operation of the MT, and its data directly support the optimisation of structural dynamics to ensure the stability of the MT under complex working conditions.

The meshing accuracy was adopted as the same as that of the static analysis, and fixed constraints were applied to the bottom support position. The first four orders of the intrinsic frequency of the MTB were obtained through modal analysis, and the simulation results are shown in Fig. 7.

The analysis results show that the low-order modal characteristics of the MTB have met the basic design requirements, but the high-precision turning-milling MT needs both high static stiffness and dynamic stability in precision machining, especially when the external excitation frequency is coupled with the intrinsic frequency, the MTB will resonate and vibrate greatly, leading to shaking of machining centres and structural deformation, which seriously affects the machining accuracy of complex parts. Based on the premise that the current material properties remain unchanged, the subsequent design needs to be adjusted through the internal structure of the MTB and the corresponding parameters, targeted to enhance the modal characteristics of the MTB, so as to increase the low-order intrinsic frequency outside the excitation band, to provide kinetic protection for high-precision machining.

Through calculation, it is known that the rotational frequency of the motor of the turning and milling compound machine tool during operation is approximately 233.3 Hz, which lies between the third and fourth order intrinsic frequency. To avoid resonance during actual operation, the fourth order intrinsic frequency is selected as the optimization target. By optimizing the design of the bed, the fourth natural frequency is further increased, it can inhibit the local resonance triggered by high-frequency excitation, make up for the dynamic risks not covered by the lower-order optimisation, and improve the vibration-resistant capability of the MT in an all-round way.

Optimised design of the MTB

Optimisation of configuration selection

By observing A and B in the MTB deformation contour diagram, it can be seen that the deformation generated in these two places is small. As MT in the actual production process will produce a large number of waste chips, in order to effectively remove chips, generally in the bottom of the MTB with chip conveyor. This paper decided to cut out a rectangular hole in A, the structure can not only effectively achieve the lightweight design of the MTB, leaving space for the placement of the chip conveyor, and can effectively reduce the deformation caused by its own weight. B is the MT holder, through the static structural analysis is known that the deformation is small, so its structural strength is strong, and at the same time through the stress contour diagram can be known that its equivalent stress is far less than the permissible stress of the MTB material, which indicates that the place can be lightweight, through the different resection shape and depth of the test, and finally take the double-sided blind hole structure for the lightweight design of the tool holder. The optimised position of A and B and the optimised structure are shown in Fig. 8.

According to Fig. 5, it can be seen that the C place is the largest deformation of the MTB, and the original structure of this place is a low strength tic-tac-toe structure, and there is no large support part in its lower part, so this paper optimizes the structure of the C place. Considering the actual processing difficulty and the reliability of the optimized structure in performance, A variety of optimisation schemes are selected for this part, which are Z-shaped structure, X-shaped structure, bionic hexagonal honeycomb structure and trapezoidal structure, and its structure is shown in Fig. 9.

In order to select an optimal structural solution as the design of the internal fascia of the MTB of a high-precision turning-milling MT, the differences between the static characteristics of the above solutions are analyzed when the mass difference is not too large. By adjusting the thickness of the fascia plate of the four solutions in the modelling software and calculating the surface area of the cross-section to make them basically equal, the mass of the internal fascia plate under the four solutions is equivalently controlled to keep the same, so that the comparison of the solutions is more accurate. When optimizing at this location, the shape, thickness and distribution of the ribs need to be taken into account. If they are too thick, shrinkage porosity may occur; if they are too thin or undergo sudden changes, it will increase the difficulty of filling and the risk of cracking. Therefore, the optimization needs to balance performance and process limitations.

After completing the FEA pre-processing and applying the same fixed constraints and boundary conditions, the analysis results of its four structures are shown in Table 2.

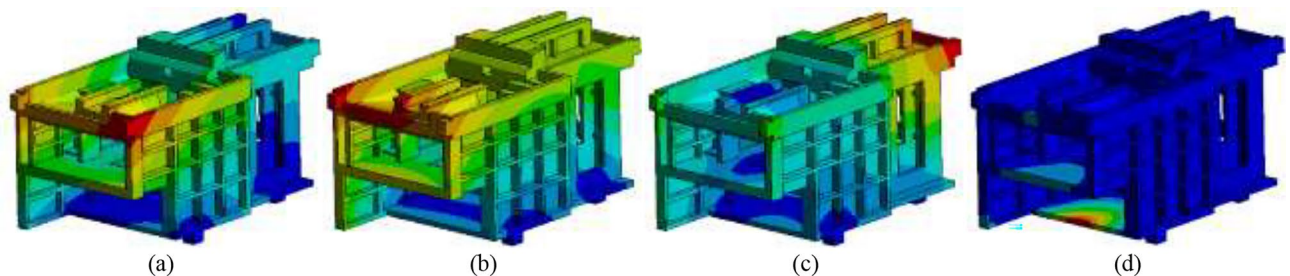


Fig. 7. Solid state frequency of the first four orders of the MTB: (a) First order intrinsic frequency: 89.31 Hz; (b) Second order intrinsic frequency: 132.72 Hz; (c) Third order intrinsic frequency: 180.85 Hz; (d) Fourth order intrinsic frequency: 264.42 Hz.

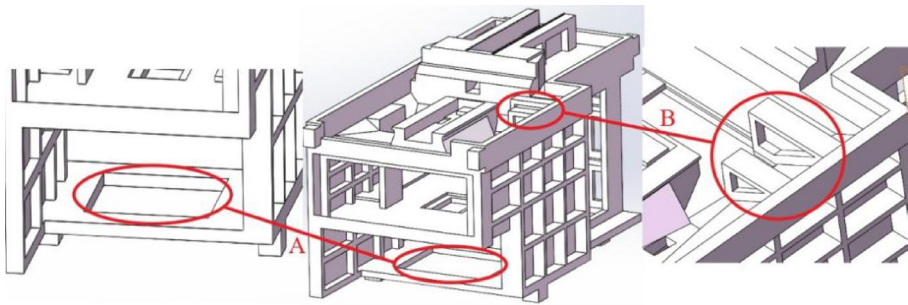


Fig. 8. Partial view of the optimised area at A and B of the MTB.

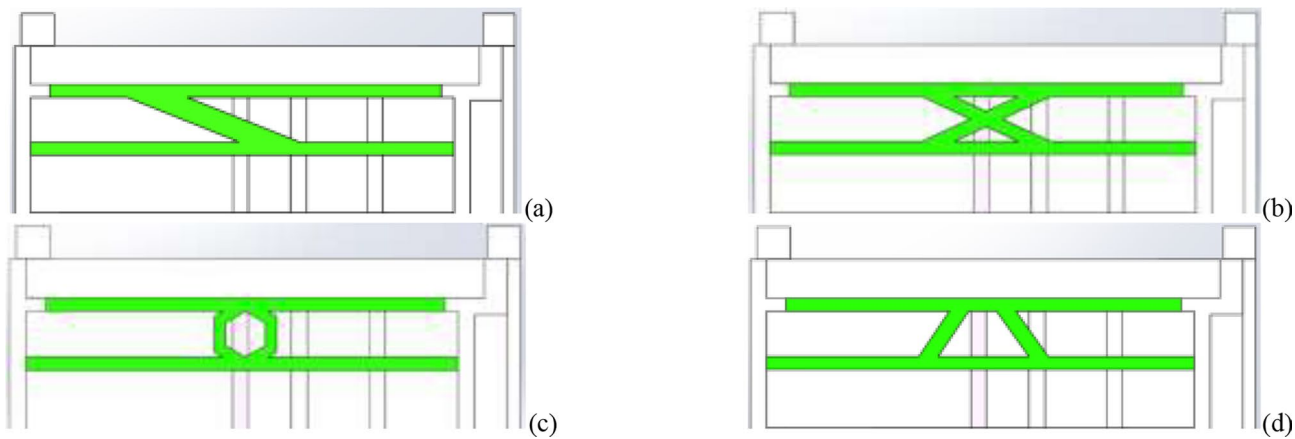


Fig. 9. Partial optimisation of the MTB(C): (a) Z-structure; (b) X-structure; (c) Biomimetic hexagonal structure; (d) Trapezoidal structure.

	Z-structure	X-structure	Biomimetic hexagonal structure	Trapezoidal structure
Deformation/ μm	9.522	9.530	9.550	9.543
Quantity/kg	1242.3	1242.9	1242	1242.8
Fourth order intrinsic frequency/Hz	267.13	267.15	267.12	267.1

Table 2. Comparison table of optimisation results for the four scenarios.

Through the above test results, it can be seen that the Z-shaped structure is the most obvious for the optimisation of deformation, and the mass and the fourth-order intrinsic frequency are not much different from the other three schemes. Since the object of this study is the MTB of high-precision turning-milling MT, which requires high machining accuracy, the Z-shaped structure is finally selected as the optimisation scheme, and the partial view of the optimised structure is shown in Fig. 10.

Optimisation of MTB dimensions and analysis of optimisation results
Optimisation of parameter selection

In order to achieve the optimisation of the dynamic and static characteristics of MTB and lightweight design, a five-factor, three-level table was selected to determine the experimental combinations. Of the five factors as shown in Fig. 11, where the middle x_1 is the length of the rectangular hole at the bottom of the machine, x_2 is the width of the rectangular hole at the bottom of the machine, x_3 is the length of the Z-structure, x_4 is the depth of the double-sided blind hole cut-in for the small tool holder, and x_5 is the depth of the double-sided blind hole cut-in for the large tool holder, and the specific dimensions of the original model are shown in Table 3.

In the Taguchi test, the selection of factor levels needs to be based on practical feasibility, resource constraints and optimisation objectives, combining experience and pre-experimentation to determine a reasonable range. Thus, the level of the selected factor is finally determined based on the experimental situation of finite element analysis. Among them, the natural frequency is evaluated by the $(S/N)_1$ characteristic, while the mass and deformation are evaluated by the $(S/N)_3$ characteristic.

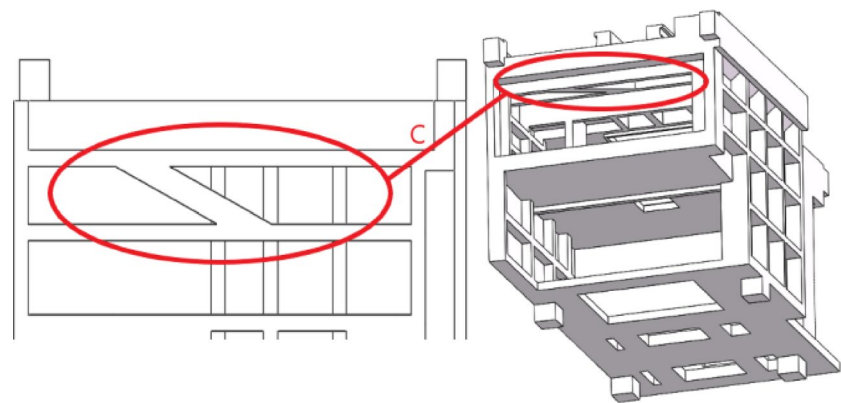


Fig. 10. Partial view of the optimised area at C of the MTB.

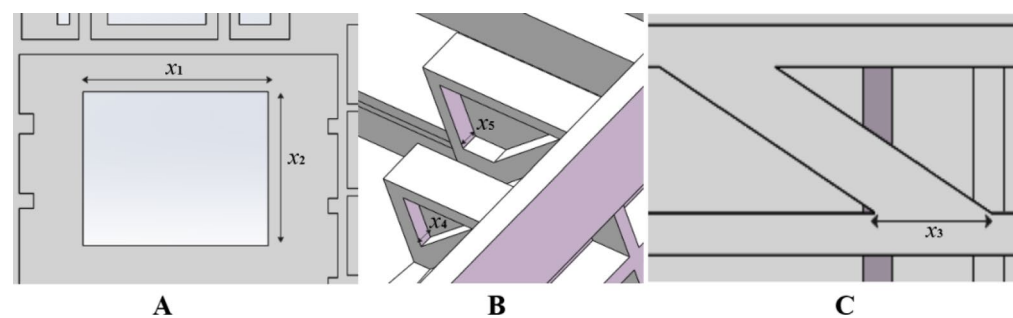


Fig. 11. Correspondence chart for each factor.

Parametric	x_1/mm	x_2/mm	x_3/mm	x_4/mm	x_5/mm
Dimension	390	310	175	15	20

Table 3. Optimisation of dimensional parameters for MTB models.

	x_1/mm	x_2/mm	x_3/mm	x_4/mm	x_5/mm
Option1	351	279	157.5	13.5	18
Option2	310	310	175	15	20
Option3	429	341	192.5	16.5	22
Option4	351	310	192.5	13.5	20
Option5	310	341	157.5	15	22
Option6	429	279	175	16.5	18
Option7	351	341	175	15	22
Option8	310	279	192.5	16.5	18
Option9	429	310	157.5	13.5	20

Table 4. Taguchi table of orthogonal tests.

Considering the instability of the actual situation, the range of values for each of the five test factors $x_i (i = 1 \sim 5)$ was taken as $(\pm 10)\%$. If the ordinary method is used, each value in this one five-parameter, three-level test is calculated individually, then at least $243(3^5)$ sets of tests will be completed. Whereas, after eliminating all the interactions using Taguchi method, the number of trials decreased to 9 sets, which significantly improved the efficiency of the trials. The orthogonal test programme for the Z-optimisation scheme is shown in Table 4 below.

	Prototype	Option1	Option2	Option3	Option4	Option5	Option6	Option7	Option8	Option9
Deformation/ μm	10.017	9.529	9.503	10.697	9.518	9.504	9.581	9.518	9.502	9.571
Quantity/kg	1273.0	1248.1	1248.6	1239.7	1246.6	1246.4	1244.4	1244.2	1250.7	1241.6
Fourth order intrinsic frequency/Hz	264.42	266.66	267.25	256.33	263.1	267.4	256.85	266.65	267.16	256.43

Table 5. Table of Taguchi orthogonal test results for MTB optimisation scheme.

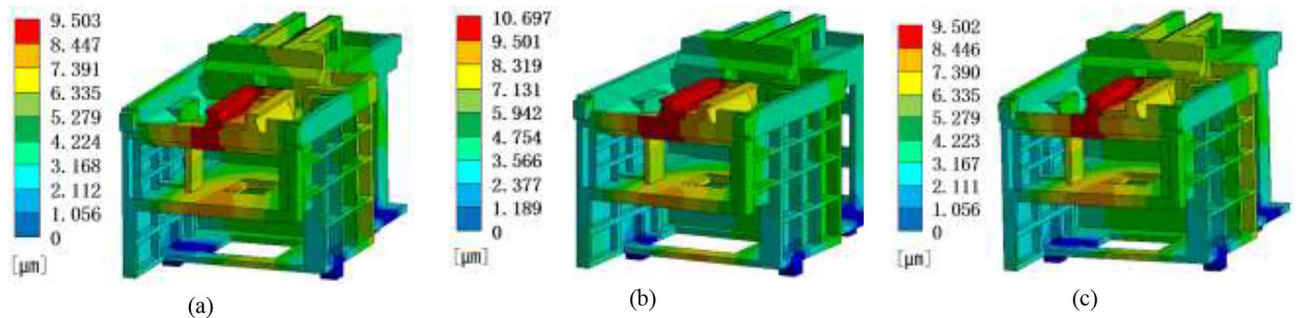


Fig. 12. Comparison of the deformation contours of the three optimisation schemes: (a) Option 2; (b) Option 3; (c) Option 8.

	Quantity/kg	Deformation/ μm	Fourth order intrinsic frequency/Hz
pre-optimisation	1273.0	10.017	264.42
post-optimisation	1250.7	9.502	267.16
rate of change	-1.75%	-5.14%	+1.04%

Table 6. Performance comparison before and after optimisation of the MTB model.

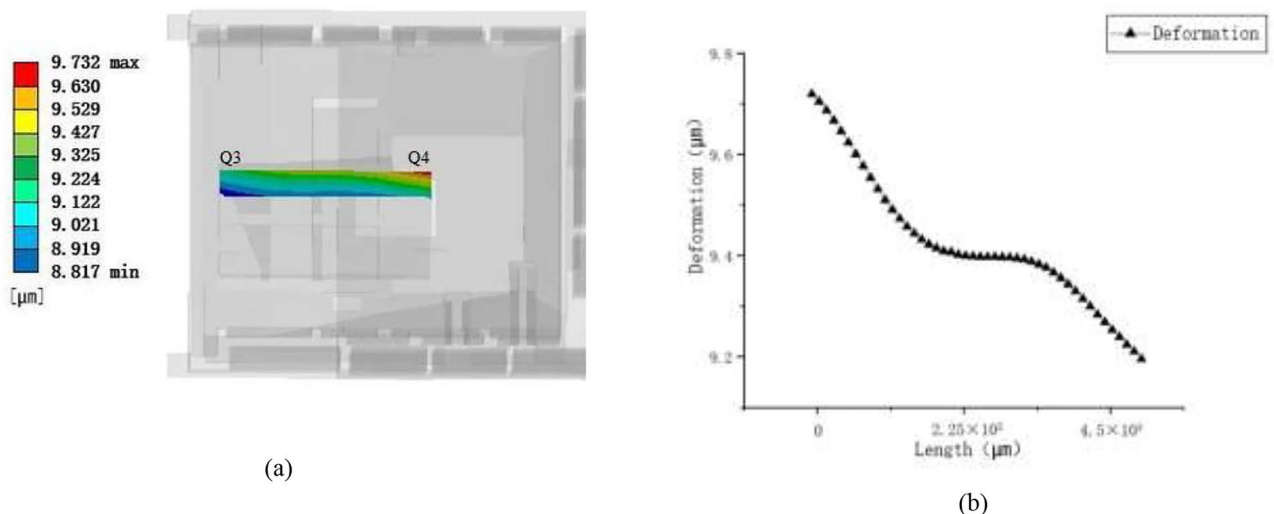


Fig. 13. Deformation contour and corresponding deformation curve of the optimised bed guides: (a) Deformation contour of the optimised bed guides; (b) Deformation curves of the bed guide rails in the Q4-Q3 direction.

Optimisation options

After finite element simulation calculations based on the Z-shaped optimisation scheme for the nine test groups in the above table by means of detailed finite element analysis, the data of their test results are obtained as shown in Table 5 below.

From the analysis results, it can be seen that Option8 is the optimal group for deformation optimisation; Option3 is the optimal group for quality optimisation; and Option2 is the optimal group for fourth-order intrinsic frequency optimisation.

Optimisation results analysis

In order to verify the reasonableness and feasibility of the optimisation of the MTB, the reconstructed model is subjected to static characteristic analysis and modal characteristic analysis. The material properties, mesh type and number, and boundary conditions of the model are kept consistent with those of the model before optimisation in the analysis. The comparative diagram of modal analysis after optimisation and the deformation contour diagram of MTB are shown in Fig. 12.

Because the multi-objective design optimisation of a MT aims to optimize several operating data of the MT and to select the most important optimisation objective to focus on. For this machine, the machine deformation is selected as the most important data in order to improve its working accuracy. The optimum deformation optimisation is chosen as Option8, while the fourth order intrinsic frequency is increased and the machine mass is reduced, which is in line with the requirements of the multi-objective optimisation. The data before and after optimisation and the rate of change are shown in Table 6 below.

As can be seen from the comparison results, after selecting scheme 8, compared with the pre-optimisation period, the fourth-order intrinsic frequency of the MTB of the turning-milling MT increases by about 1.04%, the mass decreases by about 1.75%, and the overall maximum deformation of the MTB decreases by about 5.14%.

After selecting the optimisation scheme, the deformation of the guideway under the current conditions is analyzed, and finite element analysis is carried out after controlling the variables to obtain the deformation contour diagram of the guideway of the MTB of the optimised high-precision turning-milling MT, as shown in Fig. 13.

As shown in Fig. 13(a), the deformation of the optimised bed guides is larger at the table position and smaller at the front and rear ends. Figure 13(b) shows the Z-direction deformation curve of the guideway after optimization, the maximum value of the guideway is 9.732 μm , and the minimum value is 8.817 μm . After optimization, the maximum value decreases from 10.017 μm before optimization by 0.285 μm , and the maximum deformation is reduced by 2.85%, while the minimum value decreases from 8.922 μm to 8.817 μm , which is reduced by 1.18%. After optimisation, the deformation of the guideway is reduced, and the optimisation effect is obvious, which shows that the rib layout based on the multi-objective topology optimisation scheme is effective. The reduction of guideway deformation can effectively guarantee the geometric accuracy and guiding accuracy of the table movement process, which plays an important role in improving the machining accuracy of parts.

Subsequently, monitoring paths were set up in the optimized area structures at points A, B, and C (as shown in Fig. 14), and simulation analyses and data comparisons were conducted respectively to obtain the displacement comparison curves and stress comparison curves under the specified working conditions, as shown in Figs. 15 and 16 respectively.

Under the boundary conditions studied in this paper, Fig. 15 shows the maximum axial displacement changes before and after optimization at points A, B, and C of the structure. The optimization effect at point A (Fig. 15a) is remarkable. Its maximum displacement has decreased from 7.61 μm before optimization to 6.60 μm after optimization, a reduction of 1.01 μm , with a decrease rate of 13.32%. On the contrary, the maximum displacement at point B (Fig. 15b) after optimization increased from 5.37 μm to 5.68 μm , an increase of 0.31 μm , with the same increase rate of 13.32%, indicating that the deformation at this point slightly increased. At point C (Fig. 15c), the maximum displacement after optimization shows a slight decrease, reducing from 9.80 μm to 9.57 μm , with a change of 0.23 μm and a decrease of 2.31%. In conclusion, the structural optimization effectively reduced the deformation at points A and C (particularly at point A), but led to a slight increase in the deformation at point B, and overall changed the deformation distribution characteristics of the structure.

Figure 16 shows the maximum stress changes before and after optimization at three points A, B and C of the structure. At point A (Fig. 16a), the maximum stress after optimization was 0.37 MPa, which was 0.10 MPa lower than that before optimization, with a reduction rate of 26.44%. At point B (Fig. 16b), the maximum

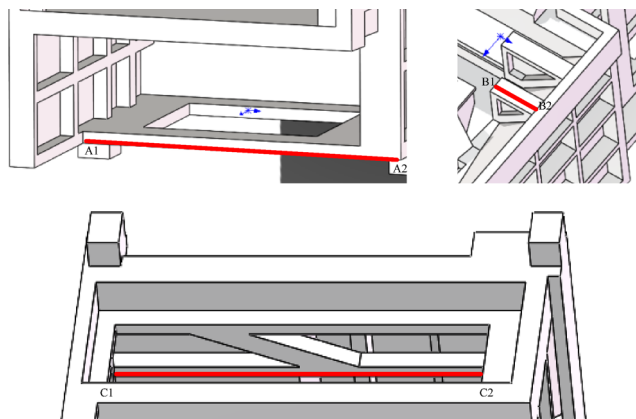


Fig. 14. Schematic diagram of the monitoring path.

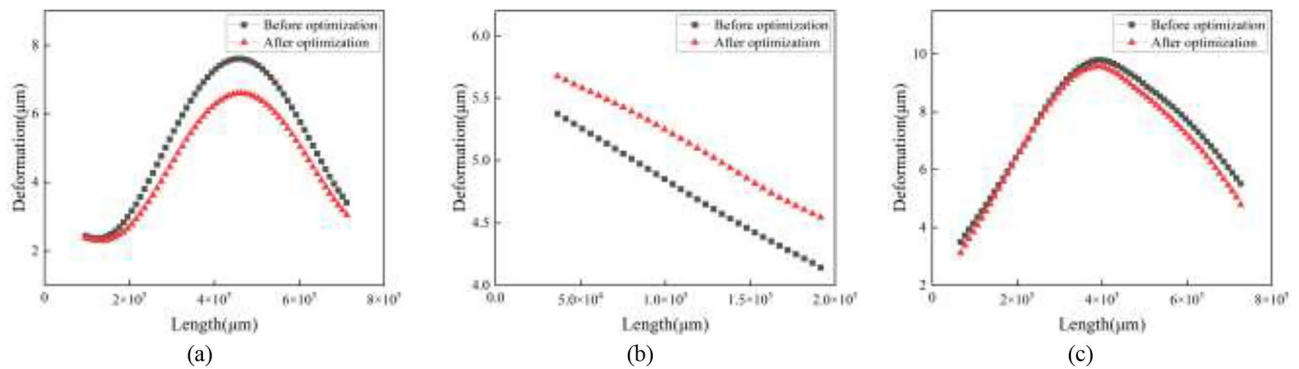


Fig. 15. The displacement comparison curve of the main optimization area: (a) Optimization Point A1-A2; (b) Optimization Point B1-B2; (c) Optimization Point C1-C2.

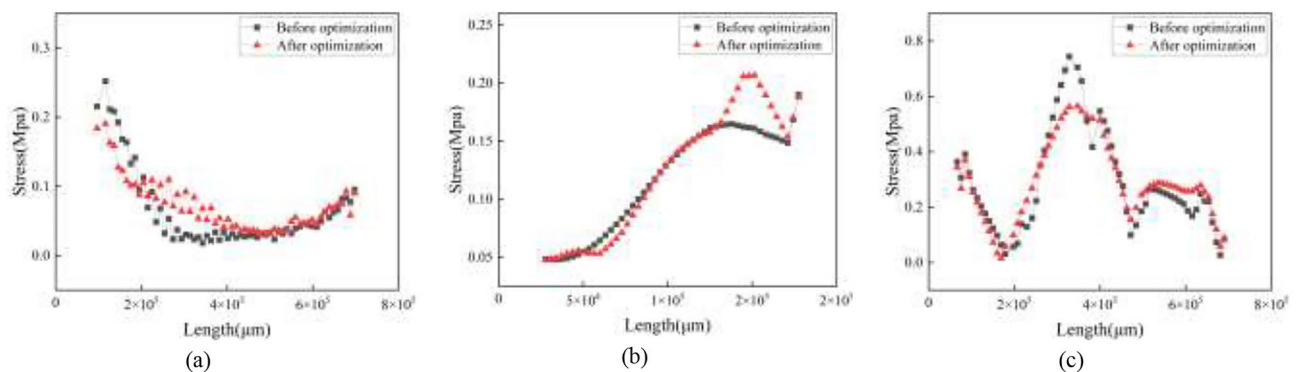


Fig. 16. The stress comparison curve of the main optimization area: (a) Optimization Point A1-A2; (b) Optimization Point B1-B2; (c) Optimization Point C1-C2.

stress after optimization is 0.22 MPa, which is 0.01 MPa lower than 0.23 MPa before optimization. At point C (Fig. 16c), the maximum stress after optimization is 0.56 MPa, which is significantly reduced by 0.23 MPa compared with 0.79 MPa before optimization. Overall, the stress variation of each main component before and after optimization did not exceed 0.1 MPa, the variation range was small, and the stress distribution at points A and C was more balanced after optimization.

In summary, the analysis results show that when conducting optimization design, the materials in the key force-bearing areas are retained and the redundancy in non-force-bearing areas are removed, the optimised MTB of the turning-milling MT is significantly improved compared with the original structure in terms of lightweight design, static mechanical performance and dynamic performance, which indicates that the new MTB structure is reasonably designed. Meanwhile, through the overall analysis of Figs. 15 and 16, it can be known that the structural changes in the optimized region have no impact on the integrity of the results. The multi-objective optimization design method proposed in this paper not only has significant advantages in optimization efficiency, but also can significantly optimize the MTB performance.

Conclusions

This study proposes a multi-objective optimization method that integrates finite element analysis (FEA) and Taguchi method in response to the demand for collaborative optimization of the dynamic and static performance of the MTB of the Turning-Milling MT. Through parametric modeling and sensitivity analysis, key design variables are precisely screened out. The Taguchi orthogonal experimental design and multi-objective joint optimization are systematically integrated to break through the efficiency bottleneck of the traditional trial-and-error method. The established “simulation - optimization - verification” technical closed loop, with FEA as the core tool, combines signal-to-noise ratio analysis to effectively balance the conflicting targets of static stiffness and dynamic characteristics, providing a new paradigm for multi-objective collaborative optimization of complex structures.

After optimisation, the MTB mass is reduced from 1273 kg to 1250.7 kg (1.75% reduction), the maximum deformation is reduced by 5.14%, and the fourth-order intrinsic frequency is increased by 1.04%, which effectively enhances the deformation resistance and dynamic stability while realizing light weight. CNC MT have demonstrated significant advantages in terms of cost, energy efficiency and productivity through the optimization of precision improvement and quality reduction. High-precision processing significantly reduces

waste and rework, further compressing operating expenses. The lightweight design reduces energy consumption, optimizes heat dissipation performance, lessens the burden on the cooling system, and aligns with the concept of green manufacturing. In addition, the combination of high precision and lightweight has enhanced processing efficiency and flexible production capacity, supporting rapid model change and multi-task processing, and promoting intelligent transformation. This optimization not only enhanced economic benefits but also facilitated the upgrading of the manufacturing industry towards high-end and green directions.

Compared with the traditional trial-and-error method, the research method in this paper shortens the optimisation cycle through systematic design variable screening and orthogonal experimental design, which demonstrates the practical engineering value. In addition, the optimisation strategy balances the relationship between static stiffness and dynamic properties, which verifies the feasibility of multi-objective co-optimisation, and the methodology can be extended to the design and optimisation of other precision MT structural components. This multi-objective joint optimization method can be extended to the design of precision machine tool structural components such as columns and headstock in the future, providing the industry with reusable optimization theoretical tools.

This study not only provides data-driven decision support for the structural design of turning-milling MT, but also establishes the 'simulation-optimisation-verification' technology route to provide a reusable theoretical framework for the dynamic design of high-precision equipment, which is of positive significance for promoting the MT industry to the direction of high-performance and intelligent development. In future work, it is possible to attempt to build a digital twin of machine tools to achieve real-time data synchronization and processing process simulation, form an intelligent optimization closed loop, and at the same time promote the system to upgrade to proactive predictive maintenance, reduce unplanned downtime, improve the overall efficiency of equipment, and lay the foundation for the construction of intelligent factories.

Data availability

The datasets used and analysed during the current study available from the corresponding author on reasonable request.

Received: 5 June 2025; Accepted: 22 July 2025

Published online: 26 July 2025

References

1. Yang, Z. J., He, J. L., Liu, Z. F., Li, G. F. & Chen, C. H. Recent progress in reliability technology of CNC machine tools[J]. *J. Mech. Eng.* **59** (19), 152–116 (2023).
2. Yang, J. S., Zhou, Z. W., Lin, X. L., Deng, X. L. & Wang, J. C. Multi-objective joint optimization design of high-precision turn-milling compound machine toolbed based on nonparametric regression response surface method[J]. *Manufacturing Technol. & Mach. Tool* **05**, 128–133 (2024).
3. Li, T. J., Ding, X. H. & Li, H. L. Research progress on lightweight design of machine tool structure[J]. *J. Mech. Eng.* **56** (21), 186–198 (2020).
4. Bruni, C., Forcellese, A., Gabrielli, F. & Simoncini, M. Hard turning of an alloy steel on a machine tool with a polymer concrete bed[J]. *J. Mater. Process. Tech.* **202** (1), 493–499 (2007).
5. Minh, P. D., Chi, T. T., Hieu, G. L., Vo, Q. A. T. & Hong, V. T. Modelling and design optimization of a novel compliant XY positioner for Vibration-Assisted CNC Milling[J]. *Machines* **12** (8), 534–534 (2024).
6. Chen, H. Y., Tang, Q. C., Li, X. Y., Yang, Y. H. & Qiao, P. Optimization of five-axis tool grinder structure based on BP neural network and genetic algorithm[J]. *Int. J. Adv. Manuf. Technol.* **133** (5–6), 2565–2582 (2024).
7. Kim, C. J., Oh, J. S., Park, C. H. & Lee, C. H. Fast flexible multibody dynamic analysis of machine tools using modal state space models[J]. *CIRP Annals - Manuf. Technol.* **72** (1), 341–344 (2023).
8. Park, S. S., Amani, S., Lee, D. Y. & Lee, J. Nam e.machine learning based substructure coupling of machine tool dynamics and chatter stability[J]. *CIRP Annals - Manuf. Technol.* **73** (1), 297–300 (2024).
9. Yasser, Z., Maria, J. O., José, A. A. & Sergio, A. Custom post-processor based on the PSO algorithm for 5 axis machine tool compensation[J]. *J. Manuf. Process.* **132**, 963–976 (2024).
10. Li, Y. T., Wu, R. R., Huang, H. & Tang, L. W. Structure design and performance simulation analysis of resin concrete machine tool column[J]. *Mech. Sci. Technol. Aerosp. Eng.* **41** (02), 192–198 (2022).
11. Li, M. X. et al. MultiObjective optimization of the design of a protective components to chassis protection module for unmanned armored vehicles.[J]. *Sci. Rep.* **15** (1), 6975 (2025).
12. Hu, L., Zha, J., Kan, F., Long, H. & Chen, Y. L. Research on a five-axis machining center worktable with bionic honeycomb lightweight structure[J]. *Materials* **14** (1), 74 (2021).
13. Xu, W. C., Jiao, J., Chen, Y., Jiang, X. W. & Wang, S. P. Analysis on design and optimization of a new vertical counter-roller spinning machine with four pairs of rollers[J]. *Forging Stamp. Technol.* **44** (01), 102–112 (2019).
14. Deng, C. Y., Yin, G. F., Fang, H. & Xiao, H. Optimal configuration of dynamic stiffness of machine tool joints based on orthogonal experiment[J]. *J. Mech. Eng.* **51** (19), 146–153 (2015).
15. Liu, S. H., Du, Y. B. & Lin, M. Study on lightweight structural optimization design system for gantry machine tool[J]. *Concur. Eng.* **27** (2), 170–185 (2019).
16. Xin, W., Zhang, Y. Y., Fu, Y., Yang, W. & Zheng, H. P. A multi-objective optimization design approach of large mining planetary gear reducer[J]. *Sci. Rep.* **13** (1), 18640 (2023).
17. Xiao, W. Q., Xu, Z. H., Bian, H. C. & Li, Z. K. Lightweight heavy-duty CNC horizontal lathe based on particle damping materials[J]. *Mechanical Syst. Signal. Processing* **147**, 107127 (2021).
18. Chan, T. C., Aman, U., Bedanta, R. & Chang, S. L. Finite element analysis and structure optimization of a gantry-type high-precision machine tool[J]. *Sci. Rep.* **13** (1), 13006 (2023).
19. Fazilat, H. D., Judith, R. M. & Richard, M. A. Statistical methods in finite element analysis[J]. *J. Biomech.* **35** (9), 1155–1161 (2002).
20. Layeb, N., Barhoumi, N., Oldal, I. & Keppler, I. Improving the strength properties of PLA acetabular liners by optimizing FDM 3D printing: Taguchi approach and finite element analysis validation[J]. *The Int. J. Adv. Manuf. Technol.* **137**(5), 1–16 (2025).
21. Özgür, V. et al. Investigation of the effects of 3D printing parameters on mechanical tests of PLA parts produced by MEX 3D printing using Taguchi method[J]. *Sci. Rep.* **15** (1), 15008 (2025).
22. Satpute, J. et al. Performance optimization for solar photovoltaic thermal system with spiral rectangular absorber using Taguchi method[J]. *Sci. Rep.* **14** (1), 23849 (2024).

23. Moaz, H. A., Ansari, M. N. M., Basim, A. K., Bashir, M. & Oshkour, A. A. Simulation machining of titanium alloy (Ti-6Al-4V) based on the finite element modeling[J]. *J. Brazilian Soc. Mech. Sci. Eng.* **36**, 315–324 (2014).
24. Cai, F. F., Ren, W. & Chen, X. X. .Optimization of cutting parameters of high speed machining for integral impeller based on Taguchi method and analysis of variance[J]. *Mach. Tool. Hydraulics.* **44** (02), 4–6 (2016).
25. Chen, W. H., Chen, C. Y., Huang, C. Y. & Hwang, C. J. Power output analysis and optimization of two straight-bladed vertical-axis wind turbines[J]. *Appl. Energy.* **185**, 223–232 (2017).
26. Selvakumar, A., Ganesan, K. & Mohanram, P. V. Dynamic analysis on fabricated mineral cast lathe bed[J]. *Proceedings of the Institution of Mechanical Engineers, Part B: Journal of Engineering Manufacture*, 227(2):261–266 (2013).
27. Sui, Y. H., Gui, P., Tang, B., Yang, H. & Lv, L. Analysis of the influence of rigid supports with different heights on the natural frequencies of machine Tools[J]. *Noise Vib. Control.* **39** (05), 18–22 (2019).

Author contributions

W H.Y., W X.Y., L H.Z wrote the main manuscript text, Y J.S. and J R.Z. prepared figures, D X.L. and W J.C provide research models to guide research ideas. All authors reviewed the manuscript.

Funding

This research was financially supported by the National Natural Science Foundation of China (52175472; 62302263), the Zhejiang Provincial Natural Science Foundation of China (LD24E050011; ZCLTGS24E0601), the Natural Science Foundation of Zhejiang Province for Distinguished Young Scholars (LR22E050002); Longyou County Competitive Science and Technology Plan Project(JHXM2023004).

Competing interests

The author(s) declared no potential conflicts of interest with respect to the research, authorship, and/or publication of this article.

Declarations

Competing interests

The authors declare no competing interests.

Additional information

Correspondence and requests for materials should be addressed to X.D.

Reprints and permissions information is available at www.nature.com/reprints.

Publisher's note Springer Nature remains neutral with regard to jurisdictional claims in published maps and institutional affiliations.

Open Access This article is licensed under a Creative Commons Attribution-NonCommercial-NoDerivatives 4.0 International License, which permits any non-commercial use, sharing, distribution and reproduction in any medium or format, as long as you give appropriate credit to the original author(s) and the source, provide a link to the Creative Commons licence, and indicate if you modified the licensed material. You do not have permission under this licence to share adapted material derived from this article or parts of it. The images or other third party material in this article are included in the article's Creative Commons licence, unless indicated otherwise in a credit line to the material. If material is not included in the article's Creative Commons licence and your intended use is not permitted by statutory regulation or exceeds the permitted use, you will need to obtain permission directly from the copyright holder. To view a copy of this licence, visit <http://creativecommons.org/licenses/by-nc-nd/4.0/>.

© The Author(s) 2025